symmetry

Article

Monitoring the Ratio of Two Normal Variables Based on Triple Exponentially Weighted Moving Average Control Charts with Fixed and Variable Sampling Intervals

Xuelong Hu [1], Guan Sun [1,*], Fupeng Xie [2] and Anan Tang [1]

[1] School of Management, Nanjing University of Posts and Telecommunications, Nanjing 210003, China; hxl0419@njupt.edu.cn (X.H.); tanganan2@sina.com (A.T.)
[2] School of Automation, Nanjing University of Science and Technology, Nanjing 210094, China; xfp@njust.edu.cn
* Correspondence: 1020112320@njupt.edu.cn; Tel.: +86-15950567942

Abstract: In statistical process control (SPC), the ratio of two normal random variables (RZ) is a valuable statistical indicator to be taken as the charting statistic. In this work, we propose a triple exponentially weighted moving average (TEWMA) chart for monitoring the RZ. Additionally, the variable sampling interval (VSI) strategy has been adopted to different control charts by researchers. With the application of this strategy, the VSI-TEWMA-RZ chart is then developed to further improve the performance of the proposed TEWMA-RZ chart. The run length (RL) properties of the proposed TEWMA-RZ and VSI-TEWMA-RZ charts are obtained by the widely used Monte-Carlo (MC) simulations. Through the comparisons with the VSI-EWMA-RZ and the VSI-DEWMA-RZ charts, the VSI-TEWMA-RZ chart is statistically more sensitive than the VSI-EWMA-RZ and the VSI-DEWMA-RZ charts in detecting small and moderate shifts. Moreover, it turned out that the VSI-TEWMA-RZ chart has better performance than the TEWMA-RZ chart on the whole. Furthermore, this paper illustrates the implementation of the proposed charts with an example from the food industry.

Keywords: SPC; RZ; EWMA chart; TEWMA chart; VSI-TEWMA chart

check for updates

Citation: Hu, X.; Sun, G.; Xie, F.; Tang, A. Monitoring the Ratio of Two Normal Variables Based on Triple Exponentially Weighted Moving Average Control Charts with Fixed and Variable Sampling Intervals. *Symmetry* **2022**, *14*, 1236. https://doi.org/10.3390/sym14061236

Academic Editors: Arne Johannssen, Nataliya Chukhrova, Quanxin Zhu, José Carlos R. Alcantud and Sergei D. Odintsov

Received: 22 April 2022
Accepted: 11 June 2022
Published: 14 June 2022

1. Introduction

The quality of products has become one of the most important factors in the company's market competition. For improving products' quality, Statistical Process Control (SPC) offers a lot of tools to supervise and control a process. Control chart, as one of the most critical tools in SPC, is often used to monitor the common or assignable causes. In the SPC literatures, control charts for monitoring the ratio of two normal random variables (RZ) have already been studied extensively. They have been used in various fields—for instance, the baking industry, the pharmaceutical industry, and the industrial production of materials, as seen in [1].

The research on the RZ control charts is mainly divided into three branches: the Shewhart type charts, the cumulative sum (CUSUM) charts and the exponentially weighted moving average (EWMA) charts. Among these three type control charts, the Shewhart control chart for monitoring the RZ was first discussed by Ref. [2], who investigated a quality control procedure for the insurance against unemployment. Ref. [3] pointed out that the distribution of the ratio was extremely complex and the statistical properties of the control chart can only be obtained by simulations. Ref. [4] put forward several guidelines to implement the Shewhart chart for supervising and controlling the ratio of glass oxide composition to its density in the glass industry. Ref. [1] discussed the Shewhart chart based on individual measurements, named as the Shewhart-RZ control chart. Following this work, Ref. [5] studied the RZ chart on the basis that subgroups consist of $n > 1$ units. Then, Ref. [6] stated that the synthetic control chart for supervising and controlling the RZ is statistically more sensitive than the Shewhart-RZ chart. As it is known to all, the Shewhart charts are ineffective in detecting small to moderate process shifts. Some researchers have suggested supplementing run rules for improving the Shewhart charts' statistical properties, see Refs. [7–9] and so on. To further improve the Shewhart-RZ chart's performance, Ref. [10] and Ref. [11] adopted the run rules to the Shewhart-RZ control charts, denoted as RR-RZ control charts for the purpose of increasing its sensitivity to small shifts.

To further overcome the shortcomings of the Shewhart-type charts in detecting a relatively small shift, some researchers have successively proposed EWMA and CUSUM charts. Both types of charts take full advantage use of the previous samples information, making charts faster in detecting relatively small shifts. For example, Refs. [12,13] proposed two one-sided EWMA-RZ charts, and it turned out that the EWMA-RZ chart is statistically more sensitive than the Shewhart -RZ chart on the whole. Additionality, Ref. [14] proposed and studied the statistical properties of two Phase II one-sided CUSUM-RZ control charts and the numerical results showed that the proposed CUSUM chart is more sensitive to small shifts than the Shewhart-RZ chart.

To further improve control charts' ability to adjust to small shifts, different methods for improving EWMA schemes have been shown in the SPC literature. These charts are considered an extension of EWMA charts. For example, Refs. [15,16] performed the exponential smoothing twice on the weighted coefficients of the EWMA charts, which was named a double exponential weighted moving average (DEWMA) chart. For more works on the DEWMA control charts, the reader may see Refs. [17,18]. Recently, Ref. [19] constructed the one-sided DEWMA chart for time between events (DEWMA-TBE) which has time-varying control limits based on the gamma distribution. It shows that the DEWMA-TBE chart is statistically more sensitive than competitors in detecting downward shifts. Moreover, Ref. [20] have improved the performance of the DEWMA-type control chart with additional run-rule schemes. Since then, Ref. [21] studied the nonparametric DEWMA chart on the basis of the Wilcoxon rank-sum test. Ref. [22] performed the exponential smoothing three times and proposed the triple exponentially weighted moving average (TEWMA) chart for monitoring a normally distributed process. Moreover, a TEWMA chart for monitoring time between events (TBE) was suggested by Ref. [23]. Recently, Ref. [24] proposed a new TEWMA chart for supervising and controlling the process dispersion, moreover the advantage of the chart is shown by comparing with some competitors in detecting small shifts. Later on, a new distribution-free TEWM chart on the basis of the Wilcoxon rank-sum statistic was proposed by Ref. [25]. The studies on the TEWMA chart have demonstrated its outstanding performance in the detection of small shifts.

In the related works of control charts, researchers have found that introducing the variable sampling interval (VSI) strategy to control charts can further improve the performance of traditional charts with a fixed sampling interval (FSI). The VSI strategy is the one that adjusts the next sampling interval based on the position of the current charting statistic on the control chart. For example, Ref. [26] proposed an EWMA-RZ chart by introducing the VSI strategy, denoted as the VSI-EWMA-RZ chart. As a result, the statistical performance of the VSI-EWMA-RZ chart is superior to the traditional EWMA-RZ charts. In addition, Ref. [27] further integrated the VSI into the CUSUM-RZ scheme, called the VSI-CUSUM-RZ chart, to enhance the CUSUM-RZ chart's performance.

Based on the above studies, it is found that the TEWMA chart has demonstrated its outstanding performance in the detection of small shifts in a normally distributed process. Motivated by this fact, this paper proposes a TEWMA chart for monitoring the RZ. Moreover, since the integration of the VSI strategy can improve the performance of the EWMA-RZ or CUSUM-RZ charts for small to moderate shifts, a VSI-TEWMA-RZ control chart is then proposed to further improve the performance of the proposed TEWMA-RZ chart.

The other parts of this paper are organized as follows: In Section 2, the distribution of the ratio Z between two normal random variables is briefly introduced. Then, the

TEWMA-RZ and VSI-TEWMA-RZ charts are introduced in next Section. Section 4 shows the design procedure of the proposed charts. The control limits and the ARL or the average time to signal (ATS) of the proposed charts are also shown in this section by using the widely used Monte-Carlo (MC) simulations. In Section 5, for different chart parameters, the performance of the VSI-TEWMA-RZ chart is compared with the TEWMA-RZ, the VSI-EWMA-RZ, and the VSI-DEWMA-RZ charts. Section 6 takes the food industry as an example and implement the proposed control chart in practice. At last, Section 7 gives several remarkable conclusions and proposals for future research works.

2. A Brief Review of the Distribution of the Ratio Z

In this section, the background of the distribution of the ratio Z is briefly outlined by considering two normally distributed random variables, X and Y—for example $\mathbf{W} = (X,Y)^T \sim N(\boldsymbol{\mu}_W, \boldsymbol{\Sigma}_W)$. Here, $\mathbf{W}$ is a bivariate normally distributed random vector with a mean vector and variance–covariance matrix, respectively, as below:

$$\boldsymbol{\mu}_W = \begin{pmatrix} \mu_X \\ \mu_Y \end{pmatrix} \tag{1}$$

$$\boldsymbol{\Sigma}_W = \begin{pmatrix} \sigma_X^2 & \rho\sigma_X\sigma_Y \\ \rho\sigma_X\sigma_Y & \sigma_Y^2 \end{pmatrix} \tag{2}$$

where ρ is the coefficient of correlation between X and Y. According to the definition, the coefficients of variation of the two random variables X and Y are defined as $\gamma_X = \frac{\sigma_X}{\mu_X}$ and $\gamma_Y = \frac{\sigma_Y}{\mu_Y}$, respectively, so the standard-deviation ratio is $\omega = \frac{\sigma_X}{\sigma_Y}$. Moreover, details of the interested ratio $Z = \frac{X}{Y}$ can refer to Refs. [28–30]. Although there is no closed-form expression for the distribution of the ratio Z, it can be approximated by applying a analogical method suggested by Refs. [5,31]. Thus, the approximated expression of the c.d.f. (cumulative distribution function) $F_Z(z \mid \gamma_X, \gamma_Y, \omega, \rho)$ of Z proposed by Ref. [5] can be obtained as follows:

$$F_Z(z \mid \gamma_X, \gamma_Y, \omega, \rho) \simeq \Phi\left(\frac{A}{B}\right), \tag{3}$$

where $\Phi(\cdot)$ is the c.d.f. of the standard normal distribution and $A = \frac{z}{\gamma_Y} - \frac{\omega}{\gamma_X}$ and $B = \sqrt{\omega^2 - 2\rho\omega z + z^2}$ are functions of z, γ_X, γ_Y, ω, and ρ. In addition, the p.d.f. (probability density function) $f_Z(z \mid \gamma_X, \gamma_Y, \omega, \rho)$ of Z can be given as follows:

$$f_Z(z \mid \gamma_X, \gamma_Y, \omega, \rho) \simeq \left(\frac{1}{B\gamma_Y} - \frac{(z-\rho\omega)A}{B^3}\right) \times \phi\left(\frac{A}{B}\right), \tag{4}$$

where $\phi\,(\cdot)$ is the p.d.f. of the standard normal distribution. The i.d.f. (inverse distribution function) $F_Z^{-1}(p \mid \gamma_X, \gamma_Y, \omega, \rho)$ of Z is,

$$F_Z^{-1}(p \mid \gamma_X, \gamma_Y, \omega, \rho) = \begin{cases} \frac{-C_2 - \sqrt{C_2^2 - 4C_1C_3}}{2C_1} & \text{if } p \in (0, 0.5], \\ \frac{-C_2 + \sqrt{C_2^2 - 4C_1C_3}}{2C_1} & \text{if } p \in [0.5, 1). \end{cases} \tag{5}$$

Here, $C_1 = \frac{1}{\gamma_Y^2} - \left(\Phi^{-1}(p)\right)^2$, $C_2 = 2\omega\left(\rho\left(\Phi^{-1}(p)\right)^2 - \frac{1}{\gamma_X\gamma_Y}\right)$ and $C_3 = \omega^2\left(\frac{1}{\gamma_X^2} - \left(\Phi^{-1}(p)\right)^2\right)$ are functions of γ_X, γ_Y, p, ω, and ρ. Moreover, $\Phi^{-1}(\cdot)$ is the i.d.f. of the standard normal distribution.

3. Construction of the TEWMA-RZ Control Charts

To implement the control chart for monitoring the ratio $Z = \frac{X}{Y}$, at each sampling point $i = 1, 2, \ldots,$ we collect independent couples $\{\mathbf{W}_{i,1}, \mathbf{W}_{i,2}, \ldots, \mathbf{W}_{i,n}\}$ and each

$\mathbf{W}_{i,j} = (X_{i,j}, Y_{i,j})^T \sim N(\boldsymbol{\mu}_{\mathbf{w},i}, \boldsymbol{\Sigma}_{\mathbf{w},i})$, $j = 1, \ldots, n$, is a bivariate normal random vector with a mean vector and variance-covariance matrix, respectively, as follows:

$$\boldsymbol{\mu}_{\mathbf{w},i} = \begin{pmatrix} \mu_{X,i} \\ \mu_{Y,i} \end{pmatrix}, \tag{6}$$

$$\boldsymbol{\Sigma}_{\mathbf{w},i} = \begin{pmatrix} \sigma^2_{X,i} & \rho_0 \sigma_{X,i}\sigma_{Y,i} \\ \rho_0 \sigma_{X,i}\sigma_{Y,i} & \sigma^2_{Y,i} \end{pmatrix}. \tag{7}$$

where ρ_0 is the defined in-control correlation coefficient between two random variables X and Y. Following Ref. [5], several assumptions are made in this paper. First, the sample units are allowed to change among subgroups, which means $\boldsymbol{\mu}_{\mathbf{w},i} \neq \boldsymbol{\mu}_{\mathbf{w},k}$ and $\boldsymbol{\Sigma}_{\mathbf{w},i} \neq \boldsymbol{\Sigma}_{\mathbf{w},k}$ for $i \neq k$. Second, for variables X and Y, there is a linear relationship, $\sigma_{X,i} = \gamma_X \times \mu_{X,i}$ and $\sigma_{Y,i} = \gamma_Y \times \mu_{Y,i}$, where γ_X and γ_Y are the supposed known and constant coefficients of the variation of X and Y, respectively. Third, the known in-control value of the ratio is $z_0 = \frac{\mu_{X,i}}{\mu_{Y,i}}$, $i = 1, 2, \ldots$ for the in-control process.

3.1. A Brief Review of the VSI-EWMA-RZ Control Chart

To improve the performance of a Shewhart-RZ chart, Ref. [26] proposed a VSI-EWMA-RZ chart for monitoring the statistic $\hat{Z}_i$,

$$\hat{Z}_i = \frac{\hat{\mu}_{X,i}}{\hat{\mu}_{Y,i}} = \frac{\overline{X}_i}{\overline{Y}_i} = \frac{\sum_{j=1}^{n} X_{i,j}}{\sum_{j=1}^{n} Y_{i,j}}, i = 1, 2, \ldots \tag{8}$$

As it has been shown in Ref. [5], the c.d.f. $F_{\hat{Z}_i}(z \mid n, \gamma_X, \gamma_Y, z_0, \rho)$ and the i.d.f $F^{-1}_{\hat{Z}_i}(p \mid n, \gamma_X, \gamma_Y, z_0, \rho_0)$ of $\hat{Z}_i$ are equal to:

$$F_{\hat{Z}_i}(z \mid n, \gamma_X, \gamma_Y, z_0, \rho) = F_Z\left(z \,\middle|\, \frac{\gamma_X}{\sqrt{n}}, \frac{\gamma_Y}{\sqrt{n}}, \frac{z_0\gamma_X}{\gamma_Y}, \rho\right), \tag{9}$$

$$F^{-1}_{\hat{Z}_i}(p \mid n, \gamma_X, \gamma_Y, z_0, \rho_0) = F^{-1}_Z\left(p \,\middle|\, \frac{\gamma_X}{\sqrt{n}}, \frac{\gamma_Y}{\sqrt{n}}, \frac{z_0\gamma_X}{\gamma_Y}, \rho_0\right), \tag{10}$$

where $F_Z\left(z \mid \frac{\gamma_X}{\sqrt{n}}, \frac{\gamma_Y}{\sqrt{n}}, \frac{z_0\gamma_X}{\gamma_Y}, \rho\right)$ is the c.d.f. of Z in Equation (3) and $F^{-1}_Z\left(p \mid \frac{\gamma_X}{\sqrt{n}}, \frac{\gamma_Y}{\sqrt{n}}, \frac{z_0\gamma_X}{\gamma_Y}, \rho_0\right)$ is the i.d.f. of Z in Equation (5).

For detecting the upward shifts, the statistic Y_i^+ of the upper-sided VSI-EWMA-RZ (denoted as VSI-EWMA-RZ$^+$) chart is defined as:

$$Y_i^+ = \max\left(z_0, (1-\lambda^+)Y^+_{i-1} + \lambda^+\hat{Z}_i\right), \; Y_0^+ = z_0, \tag{11}$$

With an upper control limit $UCL^+ = K^+ \times z_0$, where $\lambda^+ \in (0, 1]$ is the smoothing parameter and $K^+ > 1$ is chart parameter of the VSI-EWMA-RZ$^+$ chart. In addition, an upper warning limit $UWL^+ = W^+ \times z_0$ between $[z_0, UCL^+]$ is added to the chart, where $W^+ < K^+$ is the upper warning limit coefficient. A process is deemed to be out-of-control if the statistic $Y_i^+ > UCL^+$. Otherwise, the process is thought to be in-control if the statistic Y_i^+ falls within the warning region $(UWL^+, UCL^+]$, and a shorter sampling interval h_s is used to collect the next sampling point. The process is deemed to be in-control if the plotted statistic Y_i^+ falls within the safe region $[z_0, UWL^+]$, and a longer sampling interval h_L is used.

Similarly, for the detection of downward shifts, the statistic Y_i^- of the lower-sided VSI-EWMA-RZ (denoted as VSI-EWMA-RZ$^-$) chart is defined as:

$$Y_i^- = \min\left(z_0, (1-\lambda^-)Y^-_{i-1} + \lambda^-\hat{Z}_i\right), \; Y_0^- = z_0, \tag{12}$$

With a lower control limit $LCL^- = K^- \times z_0$, where $\lambda^- \in (0,1]$ is the smoothing parameter and $K^- < 1$ is the chart parameter of the VSI-EWMA-RZ$^-$ chart, respectively. In addition, a lower warning limit $LWL^- = W^- \times z_0$ between $[LCL^-, z_0]$ is added to the chart, where $W^- > K^-$ is the lower warning limit coefficient. A process is claimed to be out-of-control if the plotted statistic $Y_i^- < LCL^-$. Otherwise, the process is deemed to be in-control if the plotted statistic Y_i^- falls within the warning region $[LCL^- LWL^-)$ and a shorter sampling interval h_s is used. The process is deemed to be in-control if the plotted statistic Y_i^- falls within the safe region $[LWL^-, z_0]$ and a longer sampling interval h_L is used.

3.2. A Brief Review of the VSI-DEWMA-RZ Chart

According to Ref. [32], the one-sided VSI-DEWMA-RZ charts are constructed by making the smoothing twice and are defined as follows:

An upward VSI-DEWMA-RZ (denoted as VSI-DEWMA-RZ$^+$) chart is used to detect an increase in the process and the monitoring statistic U_i^- is:

$$Y_i^+ = \lambda^+ \hat{Z}_i + \left(1 - \lambda^+\right) Y_{i-1}^+, Y_0^+ = z_0, \tag{13}$$

$$U_i^+ = \lambda^+ Y_i^+ + \left(1 - \lambda^+\right) U_{i-1}^+, U_0^+ = z_0, \tag{14}$$

where $\lambda^+ \in (0,1]$ is the smoothing parameter and $K^+ > 1$ is the chart parameter of the VSI-DEWMA-RZ$^+$ chart, respectively. The single control limit of the chart is $UCL^+ = K^+ \times z_0$. Also, an upper warning limit $UWL^+ = W^+ \times z_0$ between $[z_0, UCL^+]$ is added, where $W^+ < K^+$ is the upper warning limit coefficient. If the plotted statistic $U_i^+ > UCL^+$, the process is considered to be out-of-control. Otherwise, the process is claimed to be in-control if $UWL^+ < U_i^+ \le UCL^+$ and a shorter sampling interval h_s is used to collect the next sampling point. The process is considered to be in-control if $z_0 \le U_i^+ \le UWL^+$ and a longer sampling interval h_L. is used. The sampling interval h_i can be expressed as follows:

$$h_i = \begin{cases} h_s, UWL^+ < U_i^+ \le UCL^+ \\ h_L,\ \ U_i^+ \le UWL^+ \end{cases} \tag{15}$$

A downward VSI-DEWMA-RZ (denoted as VSI-DEWMA-RZ$^-$) chart is used to detect a decrease in the process and the statistic U_i^- can be similarly defined as:

$$Y_i^- = \lambda^- \hat{Z}_i + \left(1 - \lambda^-\right) Y_{i-1}^-, Y_0^- = z_0, \tag{16}$$

$$U_i^- = \lambda^- Y_i^- + \left(1 - \lambda^-\right) U_{i-1}^-, U_0^- = z_0, \tag{17}$$

where $\lambda^- \in (0,1]$ and $K^- < 1$ are the smoothing and chart parameters of the FSI-DEWMA-RZ-chart, respectively. The single control limit of the chart is $LCL^- = K^- \times z_0$. A lower warning limit $LWL^- = W^- \times z_0$ between $[LCL^-, z_0]$ is added, where $W^- > K^-$ is the lower warning limit coefficient. If the plotted statistic $U_i^- < LCL^-$, the process is considered to be out-of-control. Otherwise, the process is claimed to be in-control if $LCL^- \le U_i^- < LWL^-$ and a shorter sampling interval h_s is used. The process is considered to be in-control if $LWL^- \le U_i^- \le z_0$ and a longer sampling interval h_L is used. The sampling interval h_i can be expressed in a form similar to Equation (15).

3.3. The Proposed TEWMA-RZ Charts

To further enhance the advantage of the FSI- or VSI-EWMA-RZ charts, this paper performs the exponential smoothing three times on the weighted coefficients of the EWMA charts. As the distribution of Z is non-symmetric, two separate one-sided TEWMA-RZ charts are proposed for detecting increasing and decreasing shifts, respectively. Moreover, the VSI-TEWMA-RZ chart is further proposed to increase the sensitivity of the FSI-TEWMA-RZ chart.

3.3.1. The FSI-TEWMA-RZ Chart

An upward FSI-TEWMA-RZ (denoted as FSI-TEWMA-RZ$^+$) chart is used to detect an increase in the process, and the monitoring statistic V_i^+ is:

$$Y_i^+ = \lambda^+ \hat{Z}_i + \left(1 - \lambda^+\right) Y_{i-1}^+, Y_0^+ = z_0, \tag{18}$$

$$U_i^+ = \lambda^+ Y_i^+ + \left(1 - \lambda^+\right) U_{i-1}^+, U_0^+ = z_0, \tag{19}$$

$$V_i^+ = \lambda^+ U_i^+ + \left(1 - \lambda^+\right) V_{i-1}^+, V_0^+ = z_0, \tag{20}$$

where $\lambda^+ \in (0, 1]$ is the smoothing parameter and $K^+ > 1$ is the chart parameter of the FSI-TEWMA-RZ$^+$ chart, respectively. The single control limit of the chart is $UCL^+ = K^+ \times z_0$. A process is deemed to be out-of-control if the statistic V_i^+ falls above the UCL^+. Otherwise, the process is declared to be in-control.

A downward FSI-TEWMA-RZ (denoted as FSI-TEWMA-RZ$^-$) chart is used to detect downward process sifts and the statistic V_i^- can be similarly defined as:

$$Y_i^- = \lambda^- \hat{Z}_i + \left(1 - \lambda^-\right) Y_{i-1}^-, Y_0^- = z_0, \tag{21}$$

$$U_i^- = \lambda^- Y_i^- + \left(1 - \lambda^-\right) U_{i-1}^-, U_0^- = z_0, \tag{22}$$

$$V_i^- = \lambda^- U_i^- + \left(1 - \lambda^-\right) V_{i-1}^-, V_0^- = z_0, \tag{23}$$

where $\lambda^- \in (0, 1]$ is the smoothing parameter and $K^- < 1$ is the chart parameter of the TEWMA-RZ$^-$ chart, respectively. The single control limit of the chart is $LCL^- = K^- \times z_0$. A process is deemed to be out-of-control if the charting statistic V_i^- falls below the LCL^-. Otherwise, the process is declared to be in-control.

3.3.2. The VSI-TEWMA-RZ Chart

For further enhancing the sensitivity of the FSI-TEWMA-RZ chart for small or moderate shifts in the process, this paper introduces the VSI strategy into the FSI-TEWMA-RZ control chart in Section 3.3.1.

With respect to the proposed VSI-TEWMA-RZ chart, the control limit $UCL^+(LCL^-)$ is consistent with the FSI-TEWMA-RZ chart. For the upward VSI-TEWMA-RZ (denoted as VSI-TEWMA-RZ$^+$) control chart, an upper warning limit $UWL^+ = W^+ \times z_0$ between $[z_0, UCL^+]$ is added, where $W^+ < K^+$ is the upper warning limit coefficient. If the plotted statistic $V_i^+ > UCL^+$, the process is considered to be out-of-control. Otherwise, the process is claimed to be in-control if $UWL^+ < V_i^+ \leq UCL^+$ and a shorter sampling interval h_s is used to collect the next sampling point. The process is considered to be in-control if $z_0 \leq V_i^+ \leq UWL^+$ and a longer sampling interval h_L is used. The sampling interval h_i can be expressed as follows:

$$h_i = \begin{cases} h_s, UWL^+ < V_i^+ \leq UCL^+ \\ h_L, \ \ V_i^+ \leq UWL^+ \end{cases} \tag{24}$$

In terms of the downward VSI-TEWMA-RZ (denoted as VSI-TEWMA-RZ$^-$) control chart, a lower warning limit $LWL^- = W^- \times z_0$ between $[LCL^-, z_0]$ is added, where $W^- > K^-$ is the lower warning limit coefficient. If the plotted statistic $V_i^- < LCL^-$, the process is considered to be out-of-control. Otherwise, the process is claimed to be in-control if $LCL^- \leq V_i^- < LWL^-$ and a shorter sampling interval h_s is used. The process is considered to be in-control if $LWL^- \leq V_i^- \leq z_0$ and a longer sampling interval h_L is used. The sampling interval h_i can be expressed in a form similar to Equation (24).

4. Design of the Proposed TEWMA-RZ Charts

4.1. Design of the Proposed FSI-TEWMA-RZ Chart

Because of the complexity of the charting statistic of the FSI-TEWMA-RZ chart, the run length (RL) properties of the control chart are obtained by the MC simulation in this paper. Furthermore, to evaluate the performance of the FSI-TEWMA-RZ chart, the ARL measure, which indicates the average number of samples collected before going into out-of-control state, is selected. When the process is under control, the ARL is recorded as ARL_0. Otherwise, when the process gets out of control, the ARL is recorded as ARL_1. For illustration, the detailed procedure of the MC simulation of the FSI-TEWMA-RZ$^+$ chart is summarized as follows:

Step 1 Select the values of the sample size n, the in-control ratio z_0, the smoothing parameter λ^+, and the chart coefficient K^+. Compute the corresponding control limit $UCL^+ = K^+ \times z_0$.

Step 2 Generate a random sample from a multivariate normal distribution and compute the value of the charting statistic V_i^+ as in Equation (20).

Step 3 If the charting statistic V_i^+ falls below the UCL^+, the process is deemed to be in-control and returns to Step 2. Otherwise, the process is deemed to be out-of-control and then record the RL values.

Step 4 Repeat Steps 2 and 3 for . times, calculate the ARL values from the recorded RL values. The approximated expressions of the ARL can be written as:

$$ARL = \frac{\sum_{t=1}^{N} RL_t}{N}, t = 1, \ldots, N \tag{25}$$

Without loss of generality, this paper assumes ARL_0 = 200 and further studies the ARL_1 performance of the proposed chart under different shifts. The performance of the FSI-TEWMA-RZ chart can be expressed as:

$$ARL_1 = ARL_1(n, \lambda, K, \gamma_X, \gamma_Y, z_0, \rho, \tau), \tag{26}$$

Subject to the constraint:

$$ARL(n, \lambda, K, \gamma_X, \gamma_Y, z_0, \rho, \tau = 1) = ARL_0. \tag{27}$$

When $\tau = 1$, the process is under control. Otherwise, when $\tau \neq 1$, the process is returns to be out-of-control. For the above model, considering different parameter combinations, this paper uses a bisection search algorithm to computer the value of K that satisfies the constraint of $ARL_0 = 200$, and then it is used to compute the ARL_1 values of the proposed chart.

4.2. Design of the Proposed VSI-TEWMA Charts

Since the sampling interval between the consecutive samples varies, it is not reasonable to assess the performance of the VSI-TEWMA-RZ chart by the ARL measure. Thus, the ATS is used to evaluate the performance of the VSI-TEWMA-RZ chart. The ATS represents the anticipant time before a control chart triggers an out-of-control signal. When the process is under control, it is recorded as ATS_0. Otherwise, when the process gets out-of-control, it is recorded as ATS_1.

For the FSI-TEWMA-RZ chart, the sampling interval h is fixed, which indicates that the $ATS^{FSI} = h \times ARL^{FSI}$. In general, the sampling interval of the FSI control chart is usually equal to one, that is, $h = 1$. Since the sampling interval h_i depends on the position of the currently monitoring statistic on the control chart, then the $ATS^{VSI} = E(h_i) \times ARL^{VSI}$, where $E(h_i)$ stands for the average sampling interval (ASI) of the VSI type chart. The detailed procedure of the MC simulation of the VSI-TEWMA-RZ$^+$ chart is summarized as below:

Step 1 Select the values of the sample size n, the in-control ratio z_0, the smoothing parameter λ^+, and the warning limit coefficient W^+ and K^+. Compute the corresponding warning limit $UWL^+ = W^+ \times z_0$ and the control limit $UCL^+ = K^+ \times z_0$.

Step 2 Generate a random sample from a multivariate normal distribution and compute the value of the charting statistic V_i^+ as in Equation (20).

Step 3 If $UWL^{+} < V_i^{+} \leq UCL^{+}$, a shorter sampling interval h_s is used to collect the next sampling point, and if $V_i^{+} \leq UWL^{+}$, a longer sampling interval h_L is used to collect the next sampling point. Then, the process is declared to be in-control and returns to Step 2. The times t_S and t_L of the sampling intervals h_s and h_L are recorded, respectively. Otherwise, if the V_i^{+} falls above the UCL^{+}, the process is declared to be out-of-control.

Step 4 Repeat Steps 2 and 3 for $N = 10^5$ times, calculate the ATS values from the recorded times of the sampling intervals h_s and h_L. The approximated expressions of the *ATS* can be written as:

$$ATS = h_S + h_S \times \frac{\sum_{t=1}^{N} t_S}{N} + h_L \times \frac{\sum_{t=1}^{N} t_L}{N}, t = 1, \ldots, N \tag{28}$$

Similarly, this paper assumes $ATS_0 = 200$ and further studies the ATS_1 performance of the proposed control charts under different process shifts.

The expressions of ATS^{FSI} and ATS^{VSI} are given as follows:

$$\begin{cases} ATS^{VSI} = ATS^{VSI}(n, h_S, h_L, \lambda, K, W, \gamma_0, \gamma_1, z_0, \rho, \tau) \\ ATS^{FSI} = h \times ARL_1^{FSI}(n, \lambda, K, \gamma_0, \gamma_1, z_0, \rho, \tau) \end{cases}, \tag{29}$$

For the purpose of comparing the performance of the FSI-TEWMA-RZ and the VSI-TEWMA-RZ control charts, it is necessary to make sure that the control charts have the same controlled performance. The out-of-control performance of the VSI-TEWMA-RZ chart can be expressed as below:

$$ATS_1^{VSI} = ATS_1^{VSI}(n, h_S, h_L, \lambda, K, W, \gamma_0, \gamma_1, z_0, \rho, \tau)$$

Subject to the constraint:

$$ATS_0^{VSI} = ATS_0^{FSI} \tag{30}$$

$$ASI_0 = h = 1, \tag{31}$$

where ASI_0. is the controlled ASI of the VSI-TEWMA-RZ chart. Following the research work of Ref. [33], a general formula to determine the value of h_S and h_L are as follows:

$$\rho_S h_S + \rho_L h_L = h = 1 \text{ and } \rho_S + \rho_L = 1 \tag{32}$$

where ρ_S and ρ_L are the probabilities that the statistic V_i falls into the warning area and the safe area when the process is controlled, respectively. According to the research work of Ref. [34], this paper selects $(h_S, h_L) = (0.1, 1.9)$ and $\rho_S = \rho_L = 0.5$ for illustration.

In addition, a bisection search algorithm is used to calculate the control limit coefficient K and warning limit coefficient W by satisfying the constraint of $ATS_0 = 200$ and $ASI_0 = 1$. Then, these parameters are used to calculate the out-of-control ATS_1 values for the different process shift τ. According to the research of Ref. [26], we assume $z_0 = 1$ and select $\lambda \in \{0.2, 0.5\}$ and $n \in \{1, 5\}$ to discuss the performance of the VSI-TEWMA-RZ chart. For the selected combinations of (n, λ), Table 1 shows the values of K^+ and W^+ of the VSI-TEWMA-RZ control chart. Considering the space limitation, this article only gives the values of K^+ and W^+ under the condition that $\gamma_X = \gamma_Y$. It is noted that the value of K^+ of the VSI-TEWMA-RZ chart presented in Table 1, which is the same as the one from the corresponding FSI-TEWMA-RZ chart.

Table 1. K^{+} and W^{+} values of the VSI-TEWMA-RZ chart when $ATS_0 = 200$.

λ	$(\gamma_x = 0.01, \gamma_Y = 0.01)$				$(\gamma_x = 0.2, \gamma_Y = 0.2)$			
	$n = 1$		$n = 5$		$n = 1$		$n = 5$	
	K	W	K	W	K	W	K	W
$\rho_0 = \rho_1 = -0.8$								
0.2	1.0067	0.9998	1.0030	0.9999	1.2480	1.0601	1.0762	1.0083
0.5	1.0161	1.0000	1.0071	0.9999	1.5315	1.0581	1.1699	1.0106
$\rho_0 = \rho_1 = -0.4$								
0.2	1.0059	0.9998	1.0026	0.9999	1.2061	1.0467	1.0653	1.0061
0.5	1.0141	0.9999	1.0063	1.0000	1.4454	1.0452	1.1466	1.0069
$\rho_0 = \rho_1 = 0$								
0.2	1.0050	0.9998	1.0022	0.9999	1.1618	1.0316	1.0534	1.0042
0.5	1.0119	0.9999	1.0053	1.0000	1.3544	1.0305	1.1210	1.0047
$\rho_0 = \rho_1 = 0.4$								
0.2	1.0038	0.9998	1.0017	0.9999	1.1146	1.0179	1.0397	1.0019
0.5	1.0092	0.9999	1.0041	1.0000	1.2543	1.0179	1.0912	1.0028
$\rho_0 = \rho_1 = 0.8$								
0.2	1.0022	0.9999	1.0010	1.0000	1.0574	1.0045	1.0216	1.0002
0.5	1.0053	1.0000	1.0024	1.0000	1.1316	1.0051	1.0504	1.0008

5. Numerical Results and Analysis

This section first compares the performance of the proposed VSI-TEWMA-RZ chart and the corresponding FSI-TEWMA-RZ control chart, and then compares the VSI-TEWMA-RZ chart's performance with the VSI-DEWMA-RZ chart in Ref. [32] and the VSI-EWMA-RZ chart proposed by Ref. [26]. Similar to the scenarios of Ref. [26], the parameter settings of the simulations are $\lambda \in \{0.2, 0.5\}$, $n \in \{1, 5\}$, $\gamma_X \in \{0.01, 0.2\}$, $\gamma_Y \in \{0.01, 0.2\}$ and $\rho_0 \in \{-0.8, -0.4, 0, 0.4, 0.8\}$, under different conditions $\{(\gamma_X = \gamma_Y, \rho_0 = \rho_1),\ (\gamma_X \neq \gamma_Y,\ \rho_0 = \rho_1),\ (\rho_0 \neq \rho_1, \gamma_X = \gamma_Y),\ (\rho_0 \neq \rho_1, \gamma_X \neq \gamma_Y)\}$. Since the proposed VSI-TEWMA-RZ control chart is mainly used to advance the sensitivity of the RZ chart for monitoring small shifts in a process and let us take the upward control chart for instance, we give priority to the performance of the RZ charts for the upward shifts $\tau \in \{1.001,\ 1.005,\ 1.01,\ 1.02,\ 1.05\}$.

5.1. Comparisons between the VSI-TEWMA-RZ and the FSI-TEWMA-RZ Charts

According to the above parameter settings and the values of K^{+} and W^{+} presented in Table 1, Figures 1–4 compare the performance of the upper-sided FSI-TEWMA-RZ and VSI-TEWMA-RZ charts when monitoring the upward shifts. The ARL_1 and ATS_1 represent the performances of the corresponding FSI and VSI control charts, respectively. It is pointed out that since the sampling interval of the FSI chart is $h = 1$, the FSI chart's ARL is equal to its ATS value. Then, the ARL_1 performance of the FSI chart can be directly compared with the ATS_1 performance of the VSI chart.

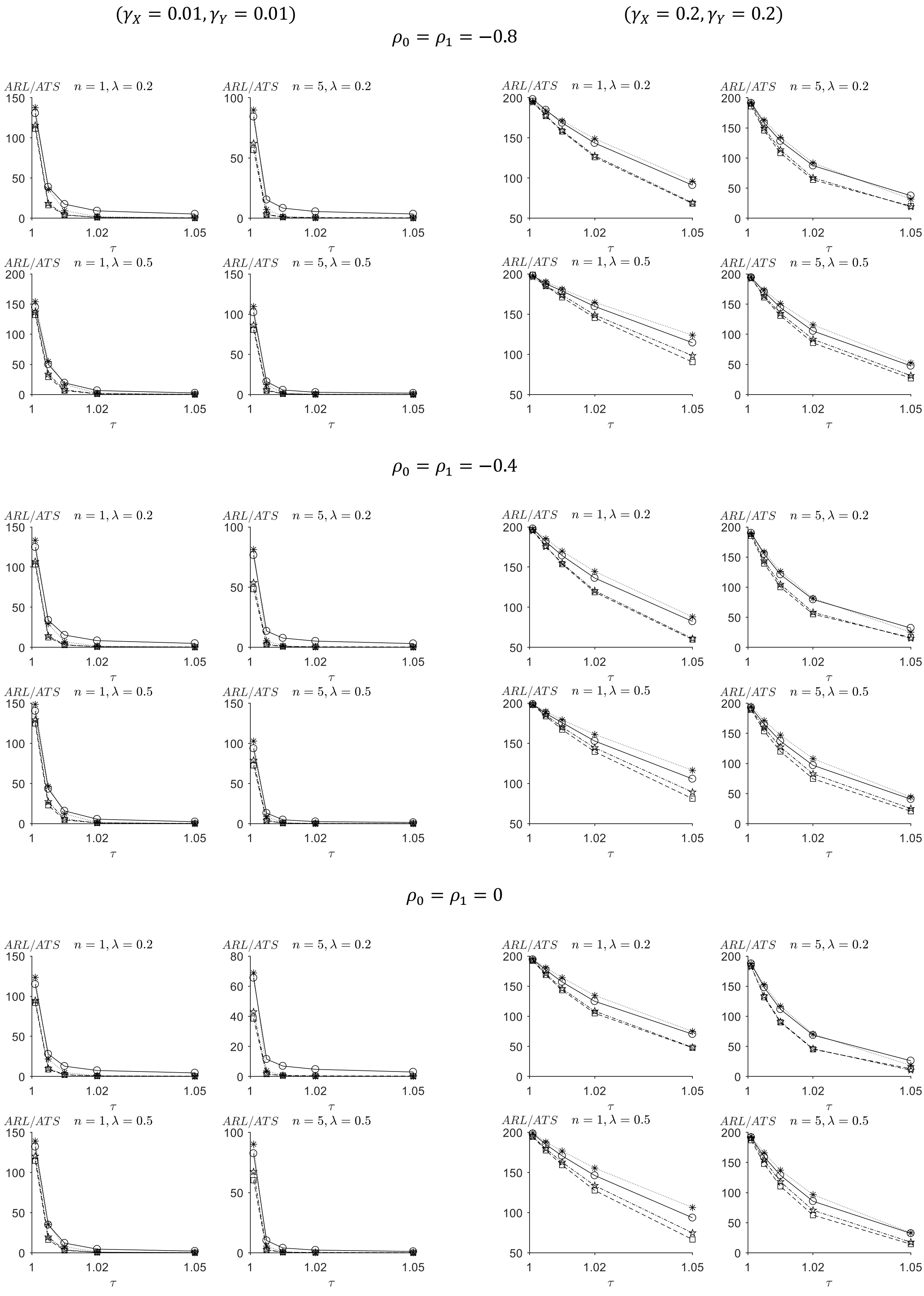

Figure 1. *Cont.*

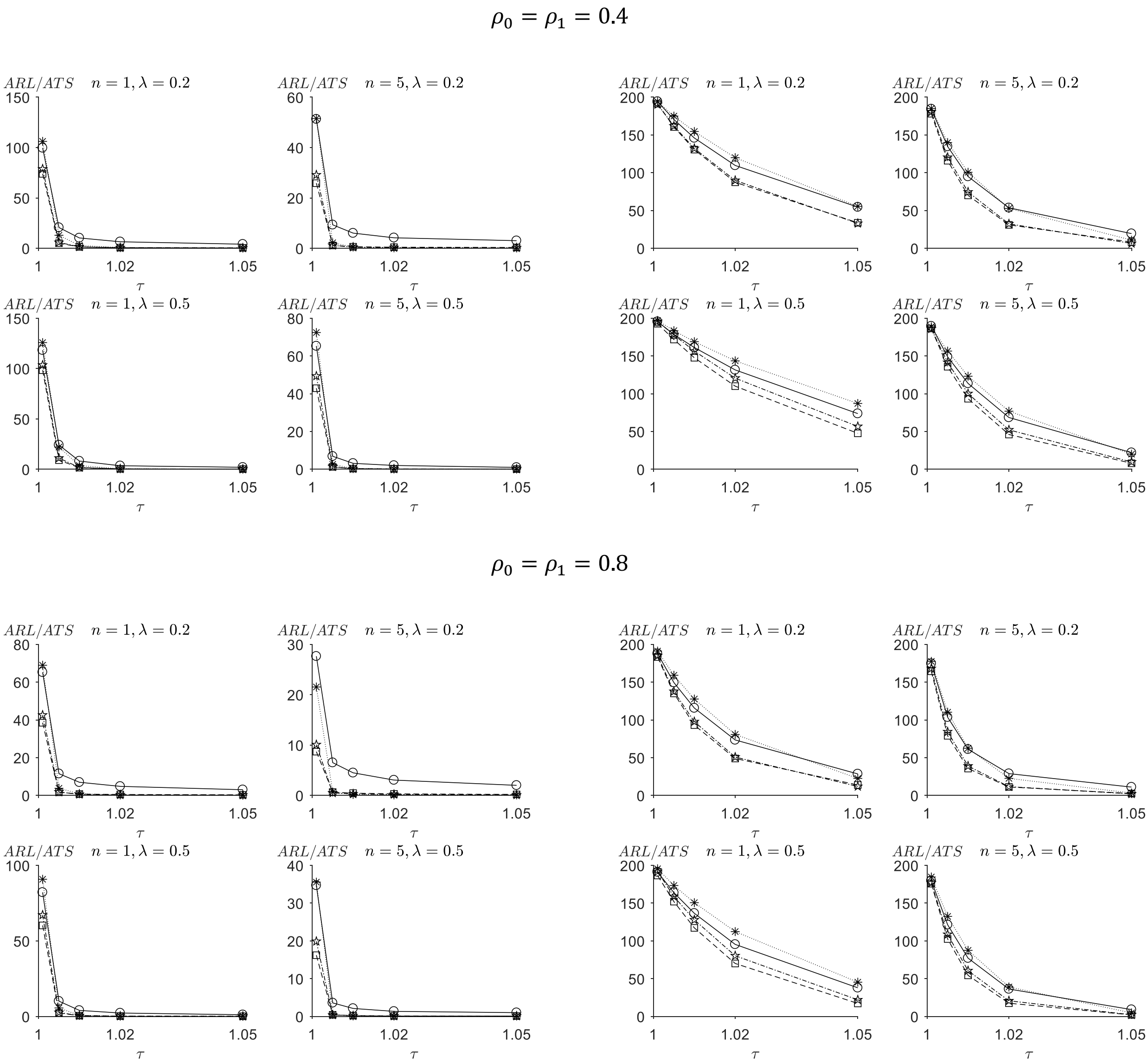

Figure 1. ARL values of the FSI-TEWMA-RZ (-○-) chart, ATS values of the VSI-DEWMA-RZ (-☆-), VSI-TEWMA-RZ (-□-), and VSI-EWMA-RZ (-⊛-) charts for $\gamma_X \in \{0.01, 0.2\}$, $\gamma_Y \in \{0.01, 0.2\}$, $\gamma_X = \gamma_Y, \rho_0 \in \{-0.8, -0.4, 0, 0.4, 0.8\}$, $\rho_0 = \rho_1$, $\tau \in \{1.001, 1.005, 1.01, 1.02, 1.05\}$ and $n \in \{1, 5\}$.

Figures 1 and 2 show the out-of-control ARL_1 values of the FSI-TEWMA-RZ and the ATS_1 values of the proposed VSI-TEWMA-RZ chart under the conditions that $(\gamma_X = \gamma_Y,\ \rho_0 = \rho_1)$ and $(\gamma_X \neq \gamma_Y,\ \rho_0 = \rho_1)$, respectively. In Figures 1 and 2, when the process is in an out-of-control state, there is no shift in the correlation between X and Y, that is $\rho = \rho_0 = \rho_1$. From the results presented in Figures 1 and 2, some conclusions can be drawn as follows:

Generally, the proposed VSI-TEWMA-RZ chart reacts faster than the proposed FSI-TEWMA-RZ chart for detecting the process shifts. For instance, when $(\gamma_X, \gamma_Y) = (0.01, 0.01)$, $n = 1$, $\lambda = 0.2$, $\tau = 1.001$, and $\rho_0 = \rho_1 = -0.8$, we obtain $ATS_1 = 111.5$ for the VSI-TEWMA-RZ chart, which is much smaller than the $ARL_1 = 130.7$ for the FSI-TEWMA-RZ chart in Figure 1.

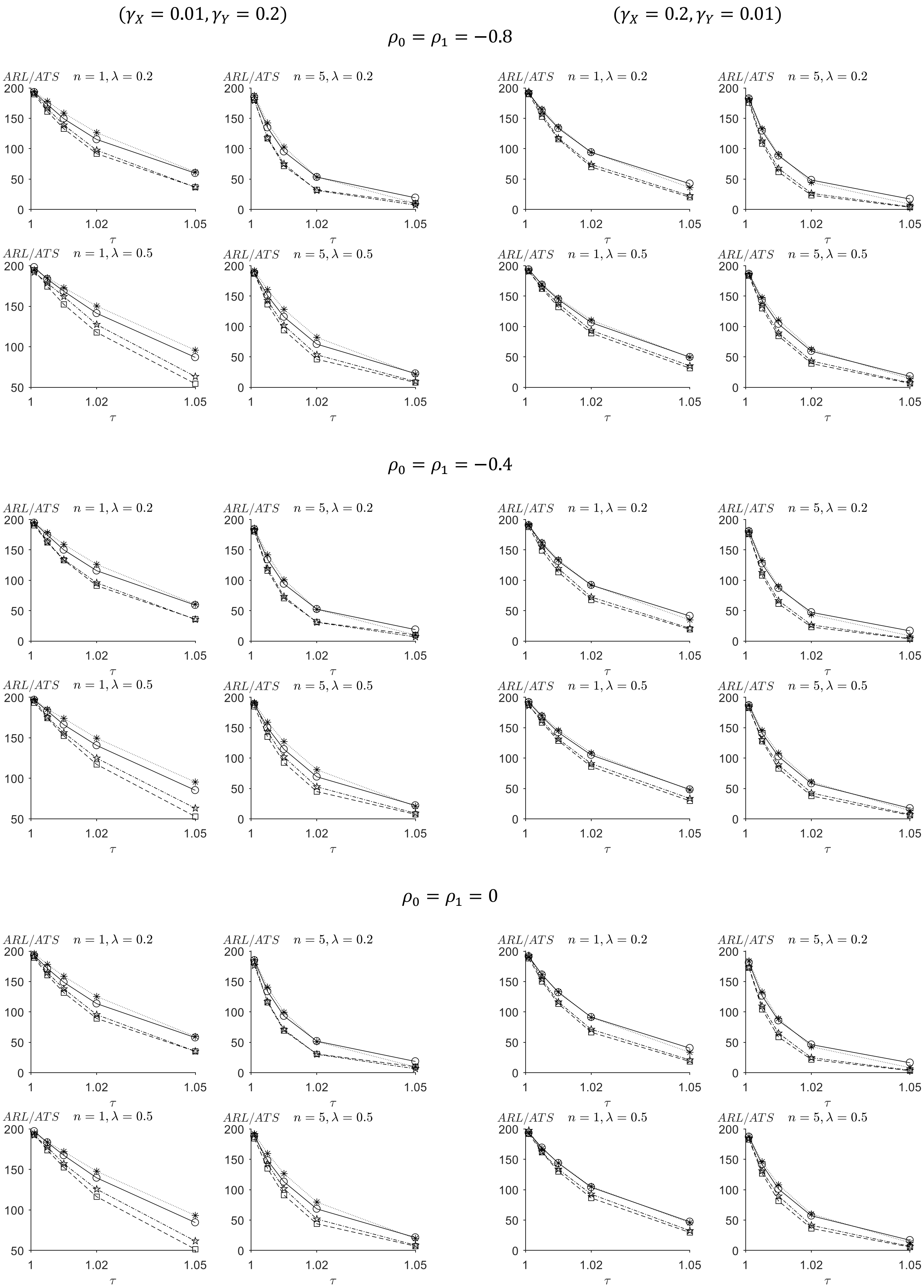

Figure 2. *Cont.*

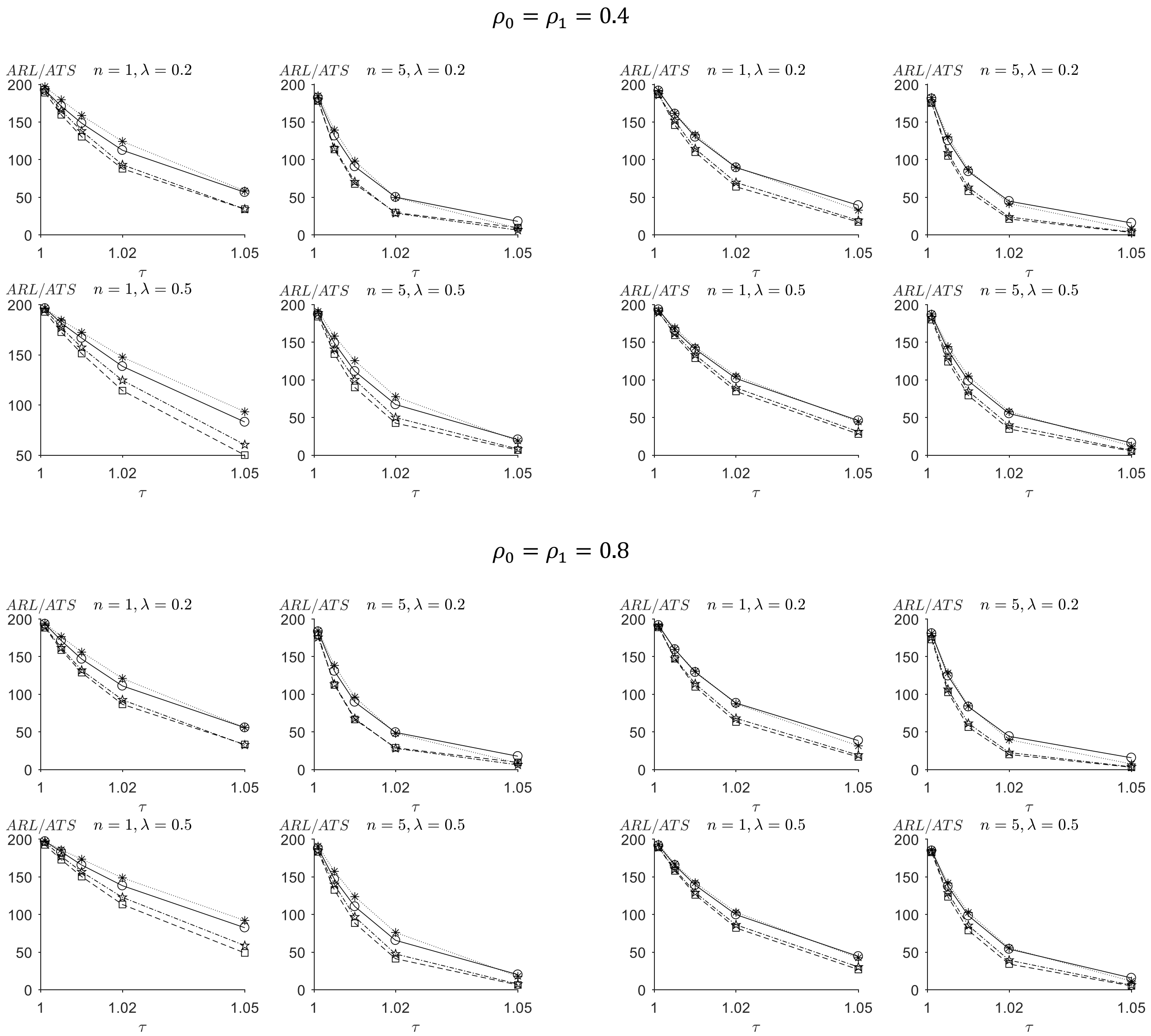

Figure 2. ARL values of the FSI-TEWMA-RZ (-○-) chart, ATS values of the VSI-DEWMA-RZ (-☆-), VSI-TEWMA-RZ (-□-), and VSI-EWMA-RZ (-⊠-) charts for $\gamma_X \in \{0.01, 0.2\}$, $\gamma_Y \in \{0.01, 0.2\}$, $\gamma_X \neq \gamma_Y$, $\rho_0 \in \{-0.8, -0.4, 0, 0.4, 0.8\}$, $\rho_0 = \rho_1$, $\tau \in \{1.001, 1.005, 1.01, 1.02, 1.05\}$ and $n \in \{1, 5\}$.

The performances of the proposed FSI- and VSI-TEWMA-RZ charts are greatly affected by (γ_X, γ_Y). When $\gamma_X = \gamma_Y$, the smaller the coefficients of variation (γ_X, γ_Y), the better the performances of the proposed FSI- and VSI-TEWMA-RZ charts. For example, when $\rho_0 = \rho_1 = 0.4$, $n = 1$, $\lambda = 0.2$, and $\tau = 1.01$ in Figure 1, we have $ATS_1 = 10.2$ for the FSI-TEWMA-RZ chart and $ATS_1 = 1.3$ for the VSI-TEWMA-RZ chart when $(\gamma_X, \gamma_Y) = (0.01, 0.01)$. As a contrast, we have $ATS_1 = 146.0$ for the FSI-TEWMA-RZ chart and $ATS_1 = 130.6$ for the VSI-TEWMA-RZ chart when (γ_X, γ_Y) increases up to $(0.2, 0.2)$.

The performances of the proposed FSI- and VSI-TEWMA-RZ charts depend on ρ_0 and ρ_1. The performances of the proposed FSI- and VSI-TEWMA-RZ charts improve when ρ_0 increases. For example, when $(\gamma_X, \gamma_Y) = (0.01, 0.01)$, $n = 1$, $\lambda = 0.5$, $\tau = 1.001$, and $\rho_0 = \rho_1 = -0.8$, we have $ATS_1 = 144.9$ for the FSI-TEWMA-RZ chart and $ATS_1 = 132.3$ for the VSI-TEWMA-RZ chart in Figure 1. As a contrast, we obtain $ATS_1 = 82.1$ for the FSI-TEWMA-RZ chart and $ATS_1 = 60.2$ when ρ_0 and ρ_1 increase up to (0.8,0.8). The performances of the proposed FSI- and VSI-TEWMA-RZ charts are influenced by λ. The FSI- and VSI-TEWMA-RZ charts have a better performance in detecting small shifts when λ is generally small. As λ increases, their ability to detect small shifts gradually deteriorates. Instead, these charts are more sensitive to large shifts. For instance, when $(\gamma_X, \gamma_Y) = (0.2, 0.2)$, $\rho_0 = \rho_1 = 0.8$, $n = 5$, and $\tau = 1.001$, we obtain $ATS_1 = 174.6$ for the FSI-TEWMA-RZ chart and $ATS_1 = 164.4$ for the VSI-TEWMA-RZ chart when $\lambda = 0.2$ in Figure 1. If λ increases up to 0.5, we obtain $ATS_1 = 179.8$ for the FSI-TEWMA-RZ chart and $ATS_1 = 175.9$ for the VSI-TEWMA-RZ chart, which are larger than the ones of the $\lambda = 0.2$ case, respectively. Moreover, for a larger shift $\tau = 1.05$, we obtain $ATS_1 = 11$ for the FSI-TEWMA-RZ chart and $ATS_1 = 2.5$ for the VSI-TEWMA-RZ chart when $\lambda = 0.2$ in Figure 1. If λ increases up to 0.5, we obtain $ATS_1 = 9.1$ for the FSI-TEWMA-RZ chart and $ATS_1 = 2.0$ for the VSI-TEWMA-RZ chart, which are smaller than the ones of the $\lambda = 0.2$ case, respectively.

Figures 3 and 4 show the ARL_1 values of the FSI-TEWMA-RZ chart and the ATS_1 values of the proposed VSI-TEWMA-RZ chart under the conditions that $(\gamma_X = \gamma_Y,\ \rho_0 \neq \rho_1)$ and $(\gamma_X \neq \gamma_Y,\ \rho_0 \neq \rho_1)$, respectively. It is worth noting that the correlation coefficient between X and Y changes, that is $\rho_0 \neq \rho_1$. In order to facilitate the comparison and to be consistent with the research of Ref. [26], this paper chooses the in-control correlation coefficient $\rho_0 = \pm 0.4$ and the values of the studied shift in the correlation are 0.5 and 2, that is $\rho_1 = 0.5 \times \rho_0$ and $\rho_1 = 2 \times \rho_0$. From Figures 3 and 4, some conclusions can be summarized as follows:

With the increase in the level of the negative correlation coefficient, that is $\rho_0, \rho_1 < 0$, $|\rho_1| > |\rho_0|$, the performances of the proposed FSI- and VSI-TEWMA-RZ charts generally improve. For instance, when $(\gamma_X, \gamma_Y) = (0.2, 0.2)$, $\rho_0 = -0.4$, $\rho_1 = 2 \times \rho_0 = -0.8$, $n = 1.$, $\lambda = 0.2$, and $\tau = 1.005$, we have $ATS_1 = 104$ for the FSI-TEWMA-RZ chart and $ATS_1 = 98.3$ for the VSI-TEWMA-RZ chart. While if $\rho_1 = \rho_0 = -0.4$, we obtain $ATS_1 = 181.6$ for the FSI-TEWMA-RZ chart and $ATS_1 = 176.3$. for the VSI-TEWMA-RZ chart. On the contrary, when the level of the negative correlation coefficient decreases, that is $|\rho_1| < |\rho_0|$ the performances of the proposed FSI- and VSI-TEWMA-RZ charts deteriorate. For example, when $\rho_1 = 0.5 \times \rho_0 = -0.2$, we obtain $ATS_1 = 273.6$ for the FSI-TEWMA-RZ chart and $ATS_1 = 272.2$ for the FSI-TEWMA-RZ chart. These ATS_1 values are all smaller than the ones of the $\rho_1 = \rho_0 = -0.4$ case, respectively.

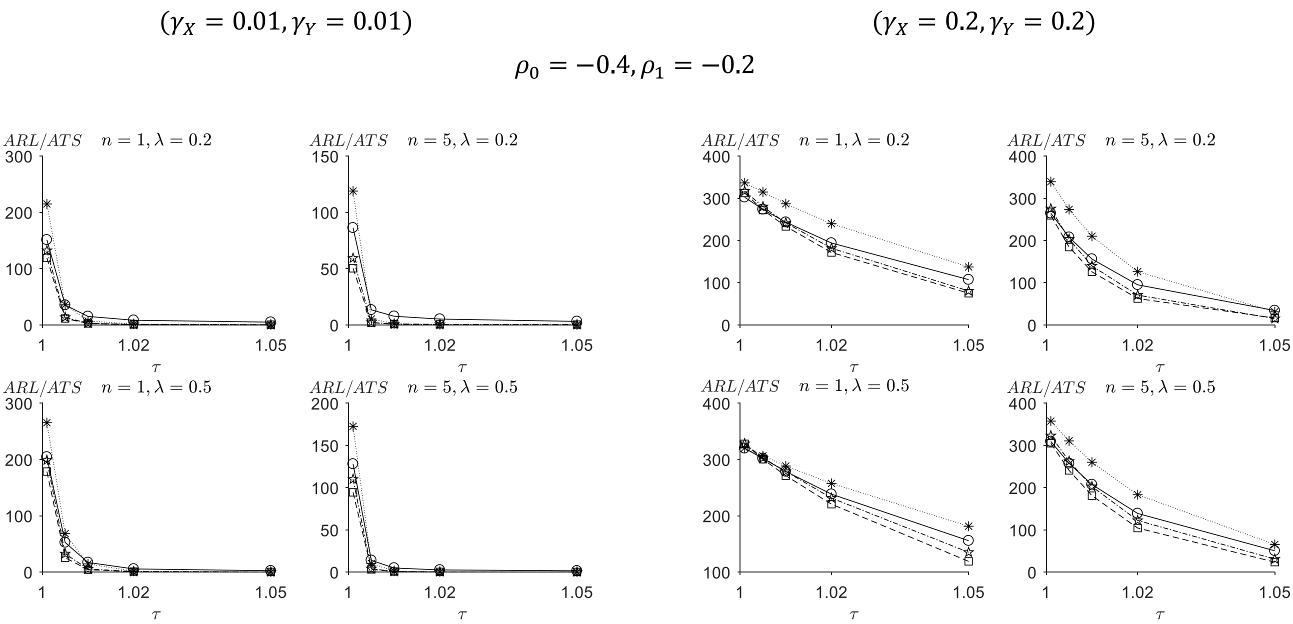

Figure 3. *Cont.*

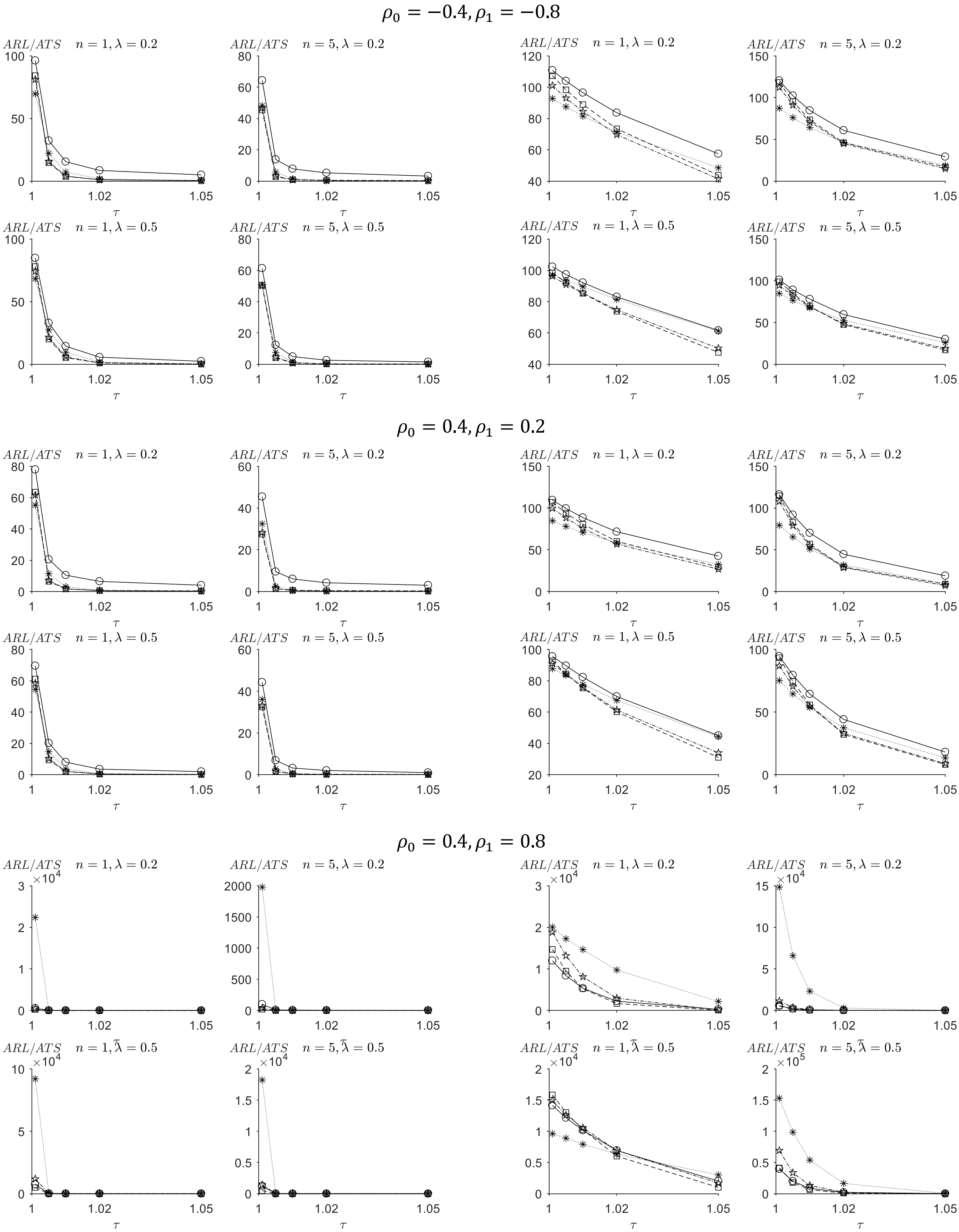

Figure 3. ARL values of the FSI-TEWMA-RZ (-○-) chart, ATS values of the VSI-DEWMA-RZ (-☆-), VSI-TEWMA-RZ (-□-), and VSI-EWMA-RZ (-⊛-) charts for $\gamma_X \in \{0.01, 0.2\}$, $\gamma_Y \in \{0.01, 0.2\}$, $\gamma_X = \gamma_Y$, $\rho_0 \in \{-0.8, -0.4, 0, 0.4, 0.8\}$, $\rho_0 \neq \rho_1$, $\tau \in \{1.001, 1.005, 1.01, 1.02, 1.05\}$ and $n \in \{1, 5\}$.

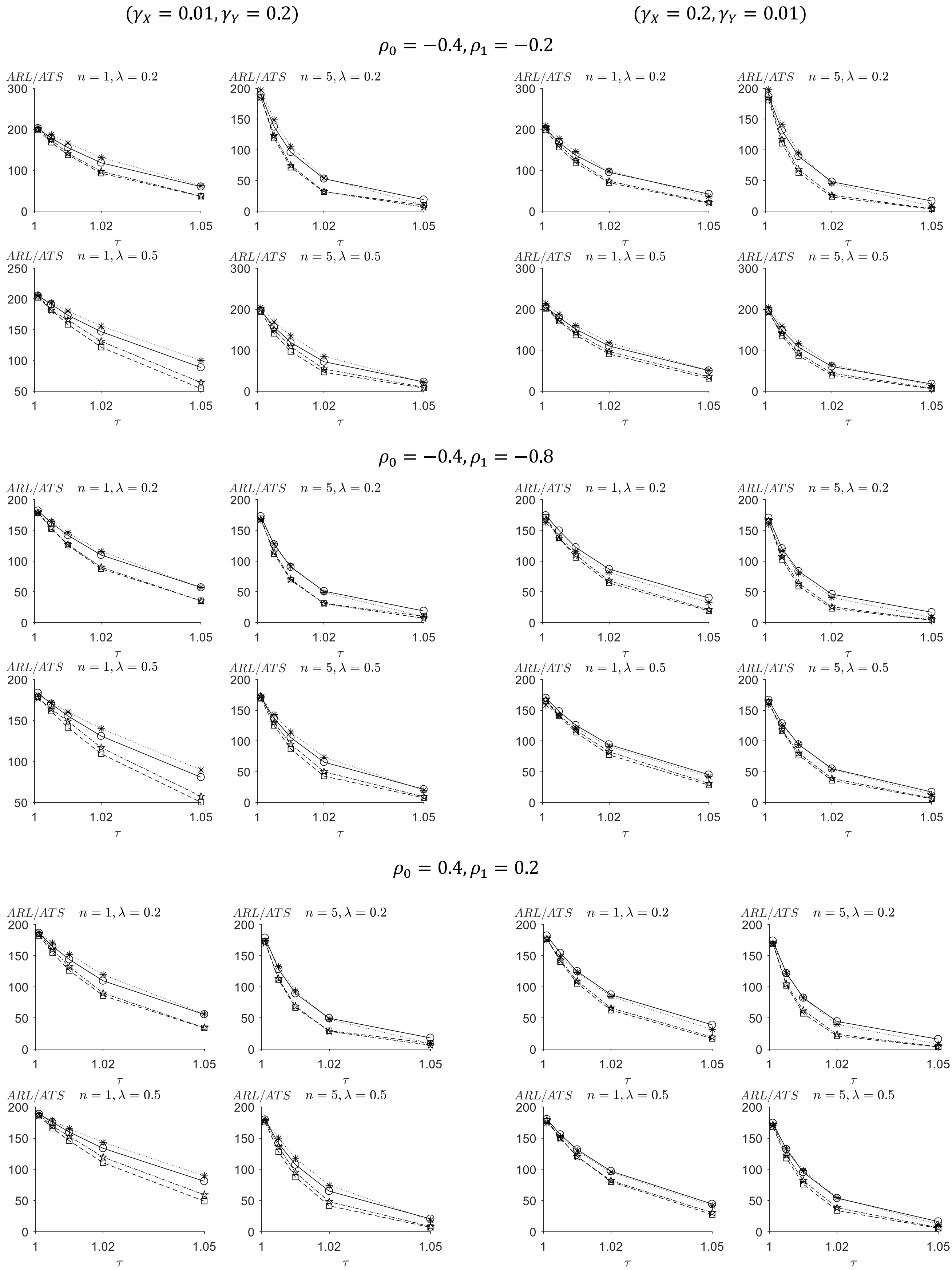

Figure 4. *Cont.*

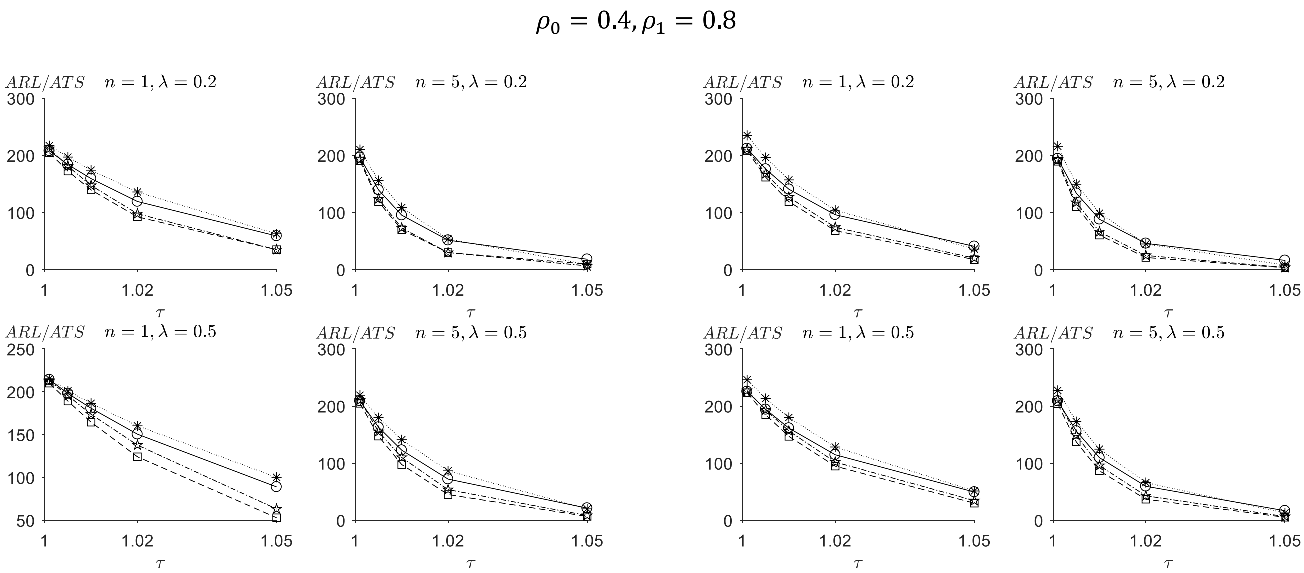

Figure 4. ARL values of the FSI-TEWMA-RZ (-○-) chart, ATS values of the VSI-DEWMA-RZ (-☆-), VSI-TEWMA-RZ (-□-) and VSI-EWMA-RZ (-⊛-) charts for $\gamma_X \in \{0.01, 0.2\}$, $\gamma_Y \in \{0.01, 0.2\}$, $\gamma_X \neq \gamma_Y$, $\rho_0 \in \{-0.8, -0.4, 0, 0.4, 0.8\}$, $\rho_0 \neq \rho_1$, $\tau \in \{1.001, 1.005, 1.01, 1.02, 1.05\}$ and $n \in \{1, 5\}$.

With the increase in the level of the positive correlation coefficient, that is when $\rho_1 > \rho_0 > 0$, the performances of the proposed FSI- and VSI-TEWMA-RZ charts generally deteriorate. For instance, when $(\gamma_X, \gamma_Y) = (0.01, 0.01)$, $\rho_1 = 2 \times \rho_0 = 0.8$, $n = 1$, $\lambda = 0.2$, $\tau = 1.001$, we have $ATS_1 = 531.9$ for the FSI-TEWMA-RZ chart and $ATS_1 = 237.6$ for the VSI-TEWMA-RZ chart. While if $\rho_1 = \rho_0 = 0.4$, we obtain $ATS_1 = 99.6$ for the FSI-TEWMA-RZ chart and $ATS_1 = 73.9$ for the VSI-TEWMA-RZ chart. On the contrary, with the decrease in the level of the positive correlation coefficient, that is when $\rho_0 > \rho_1 > 0$, the performances of the proposed FSI- and VSI-TEWMA-RZ charts improve. For instance, when $\rho_1 = 0.5 \times \rho_0 = 0.2$, we have $ATS_1 = 77.9$ for the FSI-TEWMA-RZ chart and $ATS_1 = 63.5$ for the VSI-TEWMA-RZ chart. These ATS_1 values are all smaller than the ones of the $\rho_1 = \rho_0 = 0.4$ case, respectively.

5.2. Comparisons between the VSI-TEWMA-RZ Chart and the VSI-EWMA-RZ Chart

Similarly, based on the above parameter settings and the values of K^+ and W^+ presented in Table 1, Figures 1–4 also compare the performances of the VSI-TEWMA-RZ and VSI-EWMA-RZ control charts when monitoring the upward shifts. Figures 1 and 2 present the out-of-control ATS_1 values of the VSI-EWMA-RZ chart for the condition $\rho_0 = \rho_1$. While for the condition $\rho_0 \neq \rho_1$, the ATS_1 values of the VSI-EWMA-RZ chart are shown in Figures 3 and 4. Some conclusions can be drawn from Figures 1–4.

The proposed VSI-TEWMA-RZ control chart outperforms the VSI-EWMA-RZ control chart in the detection of the upward shifts for most cases, especially for small shifts. For instance, when $\rho_0 = \rho_1$ and $(\gamma_X, \gamma_Y) = (0.01, 0.01)$ in Figure 1, the VSI-TEWMA-RZ control chart has a better performance than the VSI-EWMA-RZ control chart for the shift $\tau \in [1.001, 1.005]$. On the contrary, the VSI-EWMA-RZ chart performs better than the VSI-TEWMA-RZ chart for the detection of a relatively large shift. For instance, when $n = 5$, $\lambda = 0.2$, $\rho_0 = -0.8$, $(\gamma_X, \gamma_Y) = (0.01, 0.01)$ and $\tau = 1.05$, we have $ATS_1 = 0.1$ for the VSI-EWMA-RZ chart, which is smaller than the $ATS_1 = 0.4$ for the VSI-TEWMA-RZ chart.

When the coefficient of variation γ_X or γ_Y increases, the advantage of the VSI-TEWMA-RZ chart over the VSI-EWMA-RZ chart increases. For example, when $(\gamma_X, \gamma_Y) = (0.01, 0.01)$, the VSI-TEWMA-RZ chart outperforms the VSI-EWMA-RZ chart only for the shift range $\tau \in [1.001, 1.005]$ in Figure 1. While if (γ_X, γ_Y) increase up to $(0.2, 0.2)$, the VSI-TEWMA-RZ chart outperforms the VSI-EWMA-RZ chart for all the upward shifts.

5.3. Comparisons between the VSI-TEWMA-RZ Chart and the VSI-DEWMA-RZ Chart

Furthermore, the proposed VSI-TEWMA-RZ is compared with the VSI-DEWMA-RZ chart when monitoring the upward shifts. It can be seen from Figures 1–4 that the proposed VSI-TEWMA-RZ chart is statistically more sensitive than the VSI-DEWMA-RZ chart for detecting the process shifts, especially for small shifts. For example, when $\rho_0 = \rho_1$ and $(\gamma_X, \gamma_Y) = (0.01, 0.01)$ in Figure 1, the VSI-TEWMA-RZ control chart has a better performance than the VSI-DEWMA-RZ chart for the shift $\tau \in [1.001, 1.005]$. On the contrary, the VSI-DEWMA-RZ chart is statistically more sensitive than the VSI-TEWMA-RZ chart for the detection of a relatively large shift. For instance, when $n = 5$, $\lambda = 0.2$, $\rho_0 = -0.4$, $(\gamma_X, \gamma_Y) = (0.01, 0.2)$, and $\tau = 1.1$ in Figure 2, we have $ATS_1 = 6.8$ for the VSI-DEWMA-RZ chart, which is smaller than the $ATS_1 = 10$ for the VSI-TEWMA-RZ chart.

It can be observed that when λ increases from 0.2 to 0.5, the advantage of the VSI-TEWMA-RZ chart over the VSI-DEWMA-RZ chart increases. For instance, when $n = 5$, $\lambda = 0.5$, $\rho_0 = \rho_1 = -0.4$, and $(\gamma_X, \gamma_Y) = (0.01, 0.2)$, the VSI-TEWMA-RZ chart is statistically more sensitive than the VSI-DEWMA-RZ chart for all the upward shifts in Figure 2. However, the VSI-TEWMA-RZ chart has a better performance than the VSI-DEWMA-RZ chart for the shift $\tau \in [1.001, 1.01]$ when $\lambda = 0.2$. In addition, when the coefficient of variation γ_X or γ_Y increases, the advantage of the VSI-TEWMA-RZ chart over the VSI-EWMA-RZ chart increases. For instance, when $n = 5$ and $(\gamma_X, \gamma_Y) = (0.01, 0.01)$, the VSI-TEWMA-RZ chart outperforms the VSI-DEWMA-RZ chart for the shift range $\tau \in [1.001, 1.005]$ in Figure 1. While if (γ_X, γ_Y) increase up to $(0.2, 0.2)$, the shift range that the VSI-TEWMA-RZ chart outperforms the VSI-DEWMA-RZ chart extends to $\tau \in [1.001, 1.02]$.

6. An Illustrative Example

This section discusses the implementation of the proposed FSI- and VSI-TEWMA-RZ control charts by adopting the dataset of a muesli brand recipe discussed in Ref. [6]. This recipe was composed of several ingredients, including sunflower oil, wildflower honey, seeds (pumpkin, flaxseeds, sesame, poppy), coconut milk powder, and rolled oats. To meet the nutritional requirements recommended by the brand and preserve the flavor of the mixture, the recipe has a requirement that the weights of 'pumpkin seeds' and 'flaxseeds' be equal. Their nominal proportions to the total weight of the box content are both fixed at $p_p = p_f = 0.1$. Moreover, the brand boxes produced by the company can be packaged in 250g or 500g. To check the deviation of the controlled ratio $z_0 = \frac{\mu_{p,i}}{\mu_{f,i}} = 1$, where $\mu_{p,i}$ and $\mu_{f,i}$ are the mean weights for 'pumpkin seeds' and 'flaxseeds', respectively, at time $i = 1, 2, \ldots$, the quality practitioners wanted to perform on-line SPC monitoring and collect a sample of $n = 5$ boxes at each sampling time. Since the box size varies from one sample to another, we can obtain $\mu_{p,i} \neq \mu_{p,k}$ and $\mu_{f,i} \neq \mu_{f,k}$, $\forall i \neq k$.

In the quality control program, the 'pumpkin seeds' and 'flaxseeds' are first separated from the muesli mixture and the sample average weights $\overline{W}_{p,i} = \frac{1}{n}\sum_{j=1}^{n} W_{p,i,j}$ and $\overline{W}_{f,i} = \frac{1}{n}\sum_{j=1}^{n} W_{f,i,j}$ are recorded. At last, the ratio $\hat{Z}_i = \frac{\overline{W}_{p,i}}{\overline{W}_{f,i}}$ is calculated and plotted in the FSI- and VSI-TEWMA-RZ charts. As it has been shown in Ref. [6], for $i = 1, 2, 3 \ldots$ and $j = 1, 2, 3, \ldots$, $W_{p,i,j}$ and $W_{f,i,j}$ can be well approximated as normal variables with constant coefficients of variation $\gamma_p = 0.02$ and $\gamma_f = 0.01$, which means $W_{p,i,j} \sim N(\mu_{p,i}, 0.02 \times \mu_{p,i})$ and $W_{f,i,j} \sim N\left(\mu_{f,i}, 0.01 \times \mu_{f,i}\right)$. In addition, $\rho_0 = 0.8$ is considered as the in-control correlation coefficient between these two variables.

From an engineer's experience, a shift of 0.5% ($\tau = 1.005$) in the ratio should be interpreted as an assignable cause in the process monitoring. For this reason, we set the specified shift $\tau = 1.005$. Moreover, we chose the smoothing parameter $\lambda^+ = 0.5$ of the charts for the process monitoring. Given $n = 5$, $\lambda^+ = 0.5$, $\rho_0 = \rho_1 = 0.8$, and $(\gamma_X, \gamma_Y) = (0.02,\ 0.01)$, we obtained the control limit parameters $K^+ = 1.00497$ and $W^+ = 0.999899$ of the FSI-TEWMA-RZ$^+$ and VSI-TEWMA-RZ$^+$$K^+ = 1.009089$ and

$W^+ = 1.000779$ of the VSI-EWMA-RZ⁺ chart and $K^+ = 1.006163$ and $W^+ = 0.999942$ of the VSI-EWMA-RZ⁺ chart and z_0 is set to be 1, then $UCL^+ = K^+$ and $UWL^+ = W^+$.

Table 2 presents the set of simulated sample data collected from the process. The process is deemed to be in-control up to sample #10 and from then on, an assignable cause occurs and shifts Z_0 = 1 to $Z_1 = 1.005$. When $(h_S, h_L) = (0.1, 1.9)$, Figure 5 presents the VSI-EWMA-RZ⁺ chart, the VSI-DEWMA-RZ⁺ chart, and the FSI- and VSI-TEWMA-RZ⁺ control charts for the dataset in Table 2, where the index t in the axis is the cumulative time of the process monitoring. It can be seen from Figure 5 that the FSI- and VSI-TEWMA-RZ⁺ chart triggers an out-of-control signal at sample #15 (in bold in Table 2), while the VSI-DEWMA-RZ⁺ and VSI-EWMA-RZ⁺ charts signal an out-of-control condition at sample #16 and #18 (in bold in Table 2), respectively. This example shows that the TEWMA-RZ charts outperform the VSI-DEWMA-RZ and the VSI-EWMA-RZ charts from the perspective of the number of samples.

Table 2. The food industry example data.

Sample Number	Box Size	$W_{p,i,j}$[gr] $W_{f,i,j}$[gr]					$\overline{W}_{p,i}$[gr] $\overline{W}_{f,i}$[gr]	$\hat{Z}_i = \frac{\overline{W}_{p,i}}{\overline{W}_{f,i}}$	VSI-EWMA		VSI-DEWMA		VSI-TEWMA	
									Y_i^+	t_i	U_i^+	t_i	V_i^+	t_i
1	250 gr	25.479 25.218	25.355 25.171	24.027 24.684	25.792 25.052	24.960 25.107	25.122 25.046	1.003	1.00150	0.1	1.00075	0.1	1.00038	0.1
2	250 gr	25.359 25.211	25.172 25.115	24.508 24.679	25.292 24.933	24.449 24.831	24.956 24.954	1.000	1.00075	0.2	1.00075	0.2	1.00056	0.2
3	250 gr	24.574 24.784	24.864 24.868	25.865 25.377	25.107 24.879	24.811 24.734	25.044 24.929	1.005	1.00288	2.1	1.00181	0.3	1.00119	0.3
4	250 gr	25.313 25.338	24.483 24.859	24.088 24.305	25.184 25.115	25.681 25.251	24.950 24.974	0.999	1.00094	2.2	1.00138	0.4	1.00128	0.4
5	250 gr	25.557 25.277	24.959 25.402	25.023 25.012	24.482 24.937	25.531 25.148	25.111 25.163	0.998	1.00000	2.3	1.00042	0.5	1.00085	0.5
6	250 gr	24.882 24.962	24.473 24.644	24.814 24.817	25.418 25.419	24.732 24.818	24.864 24.932	0.997	1.00000	4.2	0.99933	0.6	1.00009	0.6
7	500 gr	49.848 49.993	48.685 49.128	49.994 49.830	49.910 49.566	49.374 49.422	49.562 49.588	0.999	1.00000	6.1	0.99897	2.5	0.99953	0.7
8	500 gr	49.668 49.695	50.338 50.681	49.149 49.640	47.807 48.969	49.064 49.612	49.205 49.720	0.990	1.00000	8	0.99664	4.4	0.99809	2.6
9	500 gr	51.273 50.366	48.303 49.210	48.510 49.844	50.594 49.890	48.591 49.595	49.454 49.781	0.993	1.00000	9.9	0.99515	6.3	0.99662	4.5
10	500 gr	48.720 49.721	51.566 50.215	49.677 50.178	50.651 50.324	50.344 50.071	50.192 50.102	1.002	1.00100	11.8	0.99649	8.2	0.99655	6.4
11	500 gr	53.173 51.081	51.079 50.660	51.636 50.468	49.187 49.787	49.779 49.197	50.971 50.239	1.015	1.00800	11.9	1.00145	10.1	0.99900	8.3
12	500 gr	51.255 49.899	48.578 49.476	49.657 49.400	49.971 49.909	50.675 50.365	50.027 49.810	1.004	1.00600	12	1.00333	10.2	1.00116	10.2
13	500 gr	48.760 48.919	50.206 50.032	51.216 50.497	51.997 50.627	49.818 49.483	50.399 49.912	1.010	1.00800	12.1	1.00547	10.3	1.00332	10.3
14	500 gr	51.599 50.351	49.257 49.885	52.077 51.044	49.874 49.898	48.791 49.506	50.319 50.137	1.004	1.00600	12.2	1.00563	10.4	1.00447	10.4
15	500gr	49.178 49.104	51.188 50.348	50.602 50.621	50.221 50.018	50.433 50.085	50.325 50.035	1.006	1.00600	12.3	1.00577	10.5	**1.00512**	**10.5**
16	500gr	50.667 50.011	50.600 49.870	50.601 49.779	49.517 50.020	50.578 49.877	50.393 49.911	1.010	1.00800	12.4	**1.00686**	**10.6**	1.00599	10.6
17	500gr	50.925 50.579	49.036 49.735	50.971 50.196	51.888 50.740	50.741 49.959	50.712 50.242	1.009	1.00850	12.5	1.00767	10.7	1.00683	10.7
18	500gr	50.673 50.459	50.653 49.990	50.346 50.281	50.749 50.251	51.338 50.281	50.752 50.252	1.010	**1.00925**	**12.6**	1.00845	10.8	1.00764	10.8
19	250gr	25.390 25.158	25.554 25.278	25.799 25.073	23.869 24.349	25.041 25.085	25.131 24.989	1.006	1.00763	12.7	1.00804	10.9	1.00784	10.9
20	250gr	24.343 24.771	26.087 25.427	25.431 25.005	24.799 24.711	26.440 25.258	25.420 25.035	1.002	1.00481	12.8	1.00642	11.0	1.00713	11.0

In the VSI-TEWMA-RZ⁺ chart, it is noted that the first six samples are in the warning region and a shorter sampling interval $h_s = 0.1$ is used to collect the next sampling point. The plotted sample point V_7^+ falls within the safe region $[z_0, UWL^+]$ and a longer sampling interval h_L is used. The VSI-TEWMA-RZ⁺ chart needs 10.5-times the units to detect the assignable cause. As a comparison, the VSI-DEWMA-RZ⁺ chart needs 10.6-times the units to trigger an out-of-control signal, while the VSI-EWMA-RZ⁺ chart needs 12.6-times the units to trigger an out-of-control signal. This shows the advantage of the VSI-TEWMA-RZ⁺ chart over the VSI-EWMA-RZ⁺ chart and VSI-DEWMA-RZ⁺ chart. Moreover, since the sampling interval of the FSI-TEWMA-RZ⁺ control chart is 1, then it needs 15-times the units to trigger an out-of-control signal. If a control chart indicates an out-of-control signal, then the quality engineering should take corrective actions to search the potential assignable causes and make the process as controlled as possible.

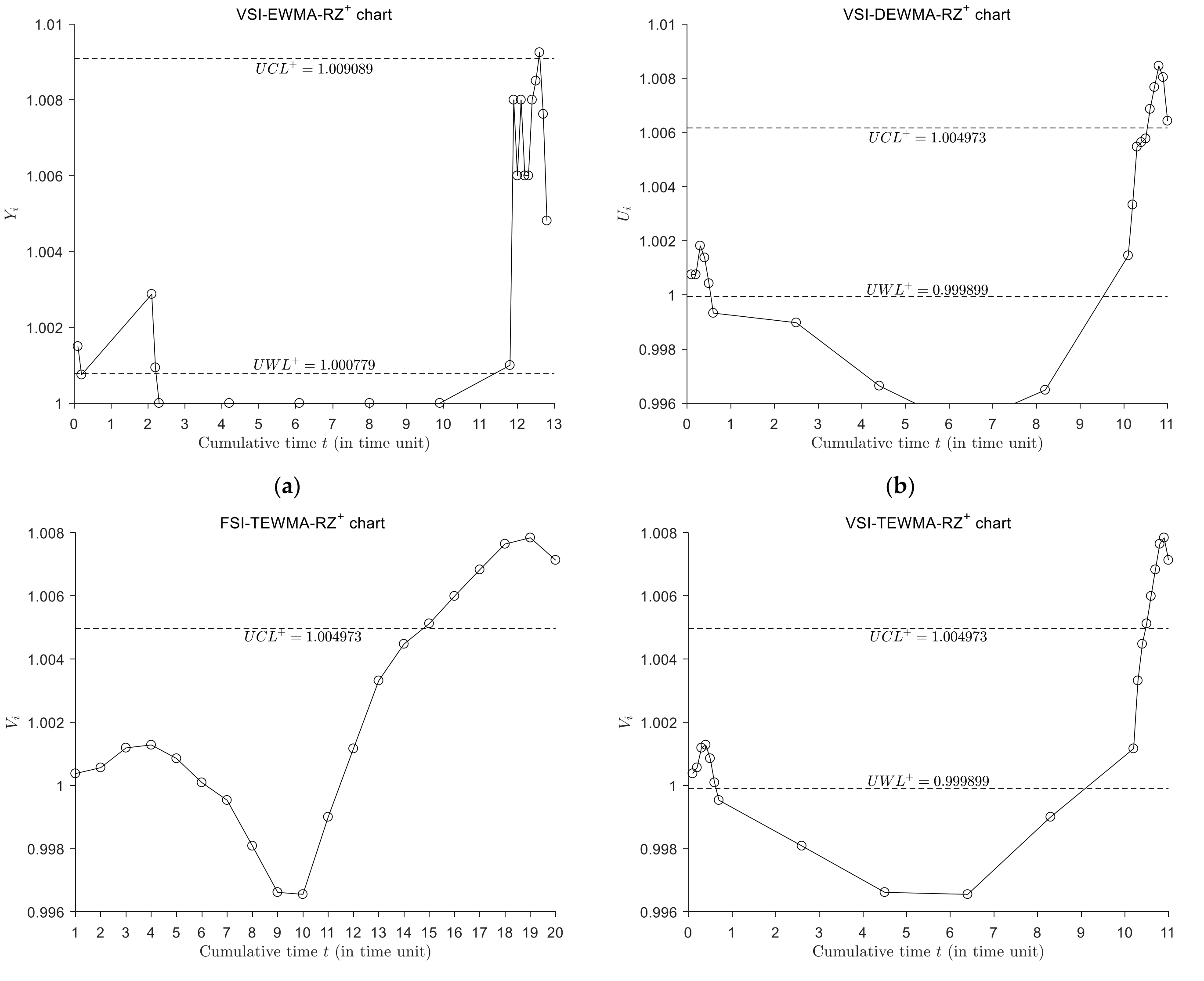

Figure 5. Different charts monitoring the food industry example. (**a**) The VSI-EWMA-RZ+ chart, (**b**) the VSI-DEWMA-RZ+ chart, (**c**) the proposed FSI-TEWMA-RZ+ chart, and (**d**) the proposed VSI-TEWMA-RZ+ charts.

7. Conclusions

In this paper, the major purpose is to propose the FSI- and VSI-TEWMA-RZ control charts by smoothing the coefficient of the EWMA-RZ chart three times. The RL properties of the proposed TEWMA-RZ charts are simulated using the MC method. Under different conditions, the performances of the VSI-TEWMA-RZ charts are presented and are compared with the FSI-TEWMA-RZ and the existing VSI-EWMA-RZ and the VSI-DEWMA-RZ charts in several figures. The results show that the performances of the proposed FSI- and VSI-TEWMA-RZ charts are greatly affected by (γ_X, γ_Y), ρ_0, and λ. Moreover, the comparison results show that the proposed VSI-TEWMA-RZ chart reacts faster than the FSI-TEWMA-RZ chart for all shifts, and the VSI-TEWMA-RZ chart also performs reacts faster than the VSI-EWMA-RZ and VSI-DEWMA-RZ charts in the detection of relatively small shifts.

Since this work is done on the assumption that both the two random variables X and Y are normally distributed, prospective research works can focus on other distributions of the two random variables to study the performance of charts for monitoring the RZ. Moreover, since some researchers have proposed distribution-free charts with the Wilcoxon rank-sum statistic, for instance Refs. [21,25,35] and so on, it would be possible to apply these distribution-free charts to monitor the RZ and study the distribution-free charts' robustness to the RZ distribution.

Author Contributions: Conceptualization, X.H. and G.S.; methodology, X.H.; software, G.S.; validation, F.X. and A.T.; formal analysis, G.S.; investigation, G.S.; resources, A.T.; data curation, X.H.; writing—original draft preparation, G.S.; writing—review and editing, X.H.; visualization, A.T.; supervision, X.H.; project administration, X.H.; funding acquisition, X.H. and A.T. All authors have read and agreed to the published version of the manuscript.

Funding: This work was supported by National Natural Science Foundation of China (Grant number: 71802110, 71671093, 72101123); China Scholarship Council (Grant number: 202006840086); The Excellent Innovation Teams of Philosophy and Social Science in Jiangsu Province (2017ZSTD022); Key Research Base of Philosophy and Social Sciences in Jiangsu Information Industry Integration Innovation and Emergency Management Research Center; Natural Science Foundation of JiangSu Province (BK20200750).

Institutional Review Board Statement: Not applicable.

Informed Consent Statement: Not applicable.

Data Availability Statement: Some or all data, models, or code generated or used during the study are available from the corresponding author by request.

Acknowledgments: This article would not have been possible without the valuable reference materials that I received from my supervisor, whose insightful guidance and enthusiastic encouragement in the course of my shaping this article definitely gain my deepest gratitude.

Conflicts of Interest: The authors declare no conflict of interest.

References

1. Celano, G.; Castagliola, P.; Faraz, A.; Fichera, S. Statistical performance of a control chart for individual observations monitoring the ratio of two normal variables. *Qual. Reliab. Eng. Int.* **2014**, *30*, 1361–1377. [CrossRef]
2. Spisak, A.W. A Control Chart for Ratios. *J. Qual. Technol.* **1990**, *22*, 34–37. [CrossRef]
3. Davis, R.B.; Woodall, W.H. Evaluation of control charts for ratios. In Proceedings of the 22nd Annual Pittsburgh Conference on Modeling and Simulation, Pittsburgh, PA, USA, 24–25 April 1975.
4. Öksoy, D.; Boulos, E.; Pye, L.D. Statistical process control by the quotient of two correlated normal variables. *Qual. Eng.* **1993**, *6*, 179–194. [CrossRef]
5. Celano, G.; Castagliola, P. Design of a phase II control chart for monitoring the ratio of two normal variables. *Qual. Reliab. Eng. Int.* **2016**, *32*, 291–308. [CrossRef]
6. Celano, G.; Castagliola, P. A synthetic control chart for monitoring the ratio of two normal variables. *Qual. Reliab. Eng. Int.* **2016**, *32*, 681–696. [CrossRef]
7. Antzoulakos, D.; Rakitzis, A. Runs rules schemes for monitoring process variability. *J. Appl. Stat.* **2010**, *37*, 1231–1247. [CrossRef]
8. Rakitzis, A.C. On the performance of modified runs rules charts with estimated parameters. *Commun. Stat. Simul. Comput.* **2017**, *46*, 1360–1380. [CrossRef]
9. Oh, J.; Wei, C.H. On the individuals chart with supplementary runs rules under serial dependence. *Methodol. Comput. Appl. Probab.* **2020**, *22*, 1257–1273. [CrossRef]
10. Tran, K.P. The efficiency of the 4-out-of-5 runs rules scheme for monitoring the ratio of population means of a bivariate normal distribution. *Int. J. Reliab. Qual. Saf. Eng.* **2016**, *23*, 1650020. [CrossRef]
11. Tran, K.P.; Castagliola, P.; Celano, G. Monitoring the ratio of two normal variables using Run Rules type control charts. *Int. J. Prod. Res.* **2015**, *54*, 1670–1688. [CrossRef]
12. Tran, K.P.; Castagliola, P.; Celano, G. Monitoring the ratio of two normal variables using EWMA type control charts. *Qual. Reliab. Eng. Int.* **2016**, *32*, 1853–1869. [CrossRef]
13. Tran, K.P.; Knoth, S. Steady-State ARL analysis of ARL-unbiased EWMA-RZ control chart monitoring the ratio of two normal variables. *Qual. Reliab. Eng. Int.* **2018**, *34*, 377–390. [CrossRef]
14. Tran, K.P.; Castagliola, P.; Celano, G. Monitoring the ratio of population means of a bivariate normal distribution using CUSUM type control charts. *Stat. Pap.* **2016**, *59*, 387–413. [CrossRef]

15. Shamma, S.E.; Amin, R.W.; Shamma, A.K. A double exponentially weigiited moving average control procedure with variable sampling intervals. *Commun. Stat.-Simul. Comput.* **1991**, *20*, 511–528. [CrossRef]
16. Shamma, S.E.; Shamma, A.K. Development and evaluation of control charts using double exponentially weighted moving averages. *Int. J. Qual. Reliab. Manag.* **1992**, *9*, 6. [CrossRef]
17. Zhang, L.; Chen, G. An extended EWMA mean chart. *Qual. Technol. Quant. Manag.* **2005**, *2*, 39–52. [CrossRef]
18. Mahmoud, M.A.; Woodall, W.H. An evaluation of the double exponentially weighted moving average control chart. *Commun. Stat. -Simul. Comput.* **2010**, *39*, 933–949. [CrossRef]
19. Alevizakos, V.; Koukouvinos, C. A double exponentially weighted moving average chart for time between events. *Commun. Stat. -Simul. Comput.* **2020**, *49*, 2765–2784. [CrossRef]
20. Adeoti, O.A.; Malela-Majika, J.-C. Double exponentially weighted moving average control chart with supplementary runs-rules. *Qual. Technol. Quant. Manag.* **2020**, *17*, 149–172. [CrossRef]
21. Malela-Majika, J.-C. New distribution-free memory-type control charts based on the Wilcoxon rank-sum statistic. *Qual. Technol. Quant. Manag.* **2021**, *18*, 135–155. [CrossRef]
22. Alevizakos, V.; Chatterjee, K.; Koukouvinos, C. The triple exponentially weighted moving average control chart. *Qual. Technol. Quant. Manag.* **2021**, *18*, 326–354. [CrossRef]
23. Alevizakos, V.; Chatterjee, K.; Koukouvinos, C. A triple exponentially weighted moving average control chart for monitoring time between events. *Qual. Reliab. Eng. Int.* **2021**, *37*, 1059–1079. [CrossRef]
24. Chatterjee, K.; Koukouvinos, C.; Lappa, A. A new S2-TEWMA control chart for monitoring process dispersion. *Qual. Reliab. Eng. Int.* **2021**, *37*, 1334–1354. [CrossRef]
25. Letshedi, T.I.; Malela-Majika, J.-C.; Castagliola, P.; Shongwe, S.C. Distribution-free triple EWMA control chart for monitoring the process location using the Wilcoxon rank-sum statistic with fast initial response feature. *Qual. Reliab. Eng. Int.* **2021**, *37*, 1996–2013. [CrossRef]
26. Nguyen, H.D.; Tran, K.P.; Heuchenne, C. Monitoring the ratio of two normal variables using variable sampling interval exponentially weighted moving average control charts. *Qual. Reliab. Eng. Int.* **2019**, *35*, 439–460. [CrossRef]
27. Nguyen, H.D.; Tran, K.P.; Heuchenne, H.L. CUSUM control charts with variable sampling interval for monitoring the ratio of two normal variables. *Qual. Reliab. Eng. Int.* **2019**, *36*, 474–497. [CrossRef]
28. Cedilnik, A.; Košmelj, K.; Blejec, A. The distribution of the ratio of jointly normal variables. *Metodoloski Zv.* **2004**, *1*, 99–108. [CrossRef]
29. Pham-Gia, T.; Turkkan, N.; Marchand, E. Density of the ratio of two normal random variables and applications. *Commun. Stat. Theory Methods* **2006**, *35*, 1569–1591. [CrossRef]
30. Oliveira, A.; Oliveira, T.; Macías, S.; Antonio. Distribution function for the ratio of two normal random variables. *AIP Conf. Proc.* **2015**, *1648*, 840005. [CrossRef]
31. Geary, R.C. The Frequency Distribution of the quotient of two normal variates. *J. R. Stat. Soc.* **1930**, *93*, 442–446. [CrossRef]
32. Sun, G.; Hu, X.; Xie, F.; Zhou, X.; Jiang, C. One-Sided double exponentially weighted moving average control charts for monitoring the ratio of two normal variables. *Sci. Iran.* **2022**. *under review*.
33. Reynolds, M.R.; Amin, R.W.; Arnold, J.C. CUSUM Charts with variable sampling intervals. *Technometrics* **1990**, *32*, 371–384. [CrossRef]
34. Haq, A.; Akhtar, S. Auxiliary information based maximum EWMA and DEWMA charts with variable sampling intervals for process mean and variance. *Commun. Stat. -Theory Methods* **2020**, *51*, 3985–4005. [CrossRef]
35. Malela-Majika, J.-C.; Rapoo, E. Distribution-free cumulative sum and exponentially weighted moving average control charts based on the Wilcoxon rank-sum statistic using ranked set sampling for monitoring mean shifts. *J. Stat. Comput. Simul.* **2016**, *86*, 3715–3734. [CrossRef]